Structure of Continuously Cooled Low-Carbon Vanadium Steels

MD. MOHAR ALI BEPARI

The structures of four 0.15 pct carbon steels containing vanadium, nitrogen, and aluminum separately and together were studied systematically, with the help of transmission electron microscopy, by cooling suitable steels at four different rates ranging from 120 °C/min to 3.6 °C/min from temperatures giving a common austenite grain size of 35 μm. Except for the steel containing only vanadium and that containing only aluminum and nitrogen cooled at the fastest rate used, the observed microstructures were all essentially mixtures of polygonal ferrite and expected amounts for pearlite. For all the steels studied, except the one containing aluminum and nitrogen, it was found that general precipitation was more common than interphase precipitation, although the extent of the latter increased at lower cooling rates. Moreover, in some cases, both general and interphase precipitation were present in the same area. The presence of aluminum was observed to enhance the formation of interphase precipitates at all cooling rates, and the spacing between parallel rows of precipitates increased as the cooling rate was decreased. The dislocation density was high at all cooling rates in all the steels, but it was found to decrease with decreasing cooling rates. Very fine precipitates were found in all the steels, except the steel containing aluminum and nitrogen. At the fast cooling rates, the segregation of vanadium and interstitial elements, which led to locally lower transformation temperatures and higher supersaturations, resulted in clusters of fine particles of vanadium carbonitride, V(C, N). At the slower cooling rates, all the steels showed severe heterogeneity in precipitate morphology which was more pronounced in the steel containing aluminum and nitrogen, while a needlelike morphology of V(C, N) precipitate was occasionally found in steels containing either vanadium and nitrogen or vanadium, nitrogen, and aluminum. As the cooling rate decreased, particle coarsening and growth occurred, causing a reduction in the number of particles/unit area. The coarsening rate of V(C, N) in the presence of aluminum is considerably lower than that of vanadium carbide, VC, or of V(C, N) in the absence of aluminum. Because of the unfavorable precipitation kinetics, any aluminum nitride (AlN) formed during cooling did not nucleate separately but was deposited on the pre-existing AlN particles, thus causing them to be coarsened very rapidly with decreasing cooling rate.

I. INTRODUCTION

VANADIUM has been added to steel for about 80 years as a means of increasing the yield strength. Its effect as a secondary hardening element is well known, and the structure of quenched and tempered mild steels containing about 1 wt pct vanadium has been reported in some detail.[1,2,3] More recently, the precipitation of vanadium carbide in isothermally transformed alloys has been studied.[4–8] The structures show another form of discontinuous precipitation in which particles are precipitated in sheets parallel to a former austenite/ferrite interphase boundary. In addition to these aspects, the effect of continuous cooling from the austenitizing temperature on the structure of vanadium steels has been examined by Tanino *et al.*[9] They found that the hardness of the alloy reached a maximum value for cooling rates of 60 °C/min to 80 °C/min. Dispersed dislocation loops and elongated dislocation dipoles, carbide particles both randomly dispersed and lined up in rows, and micro- and macrotwins were observed in foils prepared from the continuously cooled material.[9] Although recently Niltawach[10] did some work on vanadium-containing steels continuously cooled from austenitizing temperature, no systematic (detailed) study of these structures has been reported prior to the present work.

MD. MOHAR ALI BEPARI, formerly with the Department of Metallurgy, The University of Sheffield, Sheffield, England, is Professor, Department of Metallurgical Engineering, Bangladesh University of Engineering and Technology, Dhaka, Bangladesh.

Manuscript submitted December 20, 1988.

II. EXPERIMENTAL PROCEDURE

The alloys were made in an air-induction furnace, and the analyses are given in Table I. All melts were teemed at around 1600 °C, giving sound ingots of 40 kg each. All ingots were extruded to 16-mm-diameter bar at 1170 °C using a glass lubricant. The tensile specimens of each alloy from the extruded bar were solution-treated at a temperature chosen corresponding to a common austenite grain size of 35 μm,[11,12,13] as shown in Table II, for half an hour and allowed to cool to about 450 °C at four different cooling rates: 120 °C/min, 36 °C/min, 12 °C/min, and 3.6 °C/min. Below 450 °C, each specimen was allowed to cool down to ambient temperature at its natural cooling rate. A 5 kW radio frequency generator with automatic control system (programmable) was used for this purpose. The heat-treated tensile specimens were then tested to obtain data on tensile properties which have been reported elsewhere.[14]

Table I. Chemical Analysis of the Steels

Steel Number	Chemical Analysis, Wt Pct					
	C	Mn	V	N	Al	Si
2	0.15	1.42	0.22	0.005	—	0.26
3	0.15	1.52	0.20	0.020	—	0.30
4	0.15	1.57	0.20	0.024	0.056	0.30
5	0.15	1.42	—	0.020	0.053	0.19

The residuals are similar for each steel, and no element is present in an amount greater than 0.02 pct.

The structure was primarily studied by optical microscopy. The Ar_1 and Ar_3 transformation temperatures at the fast cooling rate of 120 °C/min were determined by differential dilatometry and are shown in Table III. In order to study the precipitate morphology (size, shape, and distribution) and general structural effect by transmission electron microscopy, carbon extraction replicas and thin foil discs were prepared from the heat-treated specimens. Precipitate sizes and the number of precipitates/unit area as a measure of distribution were determined in the electron micrographs taken from the extraction replicas.

III. EXPERIMENTAL RESULTS

The composition of the steels (Table I) indicates that the second-phase particles in steels 2, 3, and 5 are expected to be essentially vanadium carbide, VC, vanadium carbonitride, V(C, N), and aluminum nitride, AlN, respectively, and that those in steel 4 should be a mixture of AlN and V(C, N). These were, in fact, identified and confirmed by transmission electron microscopy, which will be discussed later.

A. *Light Optical Microscopy*

Light microscopy showed that all steels exhibited a polygonal ferrite-pearlite structure, except steels 2 and 5, at the cooling rate of 120 °C/min. At this fast cooling rate, steels 2 and 5 gave a mixed structure of bainite, pearlite, and ferrite, as shown in Figure 1, although the volume fraction of bainite in steel 2 was very small. Moreover, all the steels with this fast cooling rate showed some Widmanstätten ferrite-pearlite. Figure 2 illustrates light micrographs with the clear polygonal structure typical of all the steels cooled at 12 °C/min.

Inhomogeneities in structure and microsegregation were found in steels 2 through 4 at the cooling rate of 36 °C/min. Inhomogeneities of microstructure of the steels at this cooling rate indicate the microsegregation of alloying element (most probably manganese) in the region where the grain size was exceptionally fine.

Table II. Solution Treatment Temperature of the Steels

Steel Number	Solution Treatment Temperature (°C)
2	1025
3	1065
4	1105
5	1120

Table III. Transformation Temperature of the Steels at the Fast Cooling Rate of 120 °C/min (°C)

Steel Number	Ar_3	Ar_1
2	740	597
3	716	572
4	721	602
5	661	591

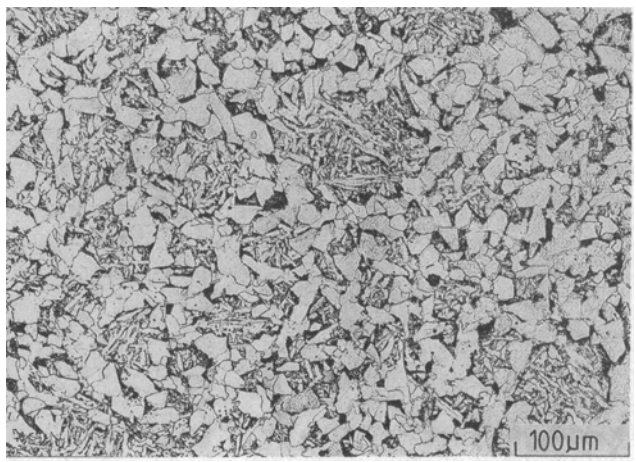

(*a*)

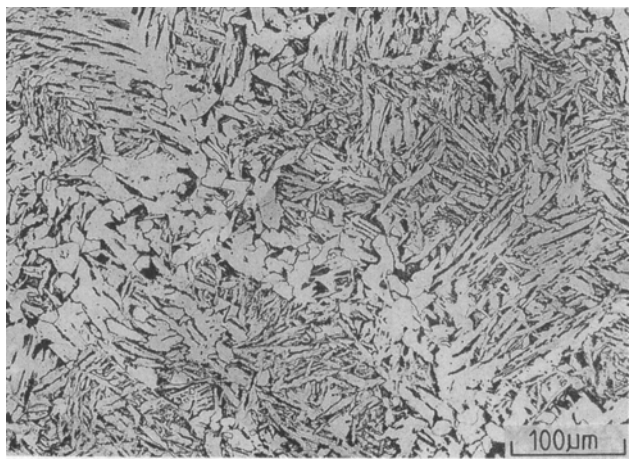

(*b*)

Fig. 1—Light micrographs of steels 2 and 5 cooled at 120 °C/min showing mixed structure of bainite, pearlite, and ferrite: (*a*) steel 2 and (*b*) steel 5.

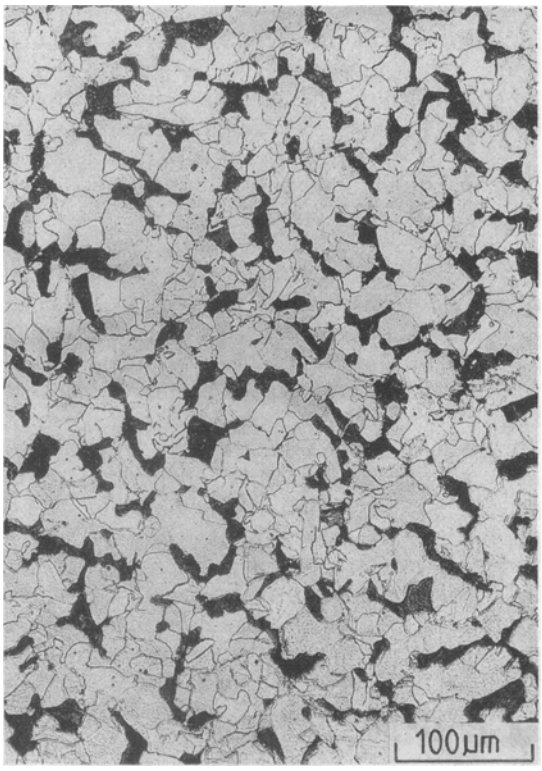

(*a*)

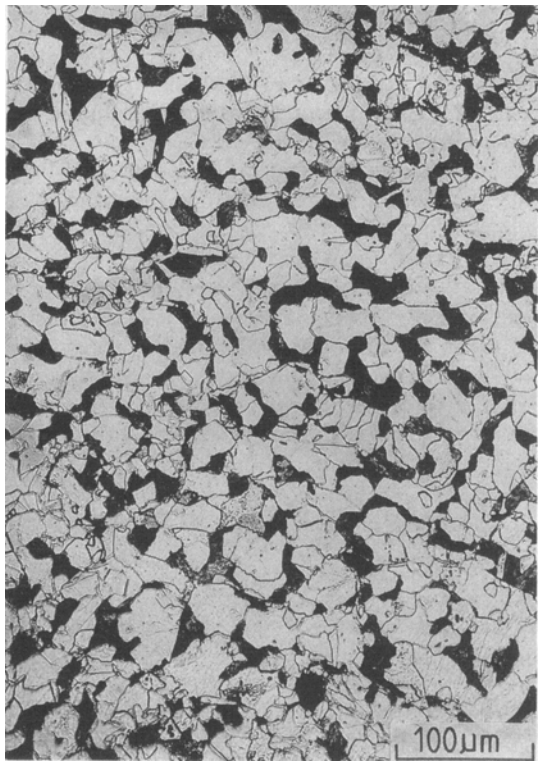

(*b*)

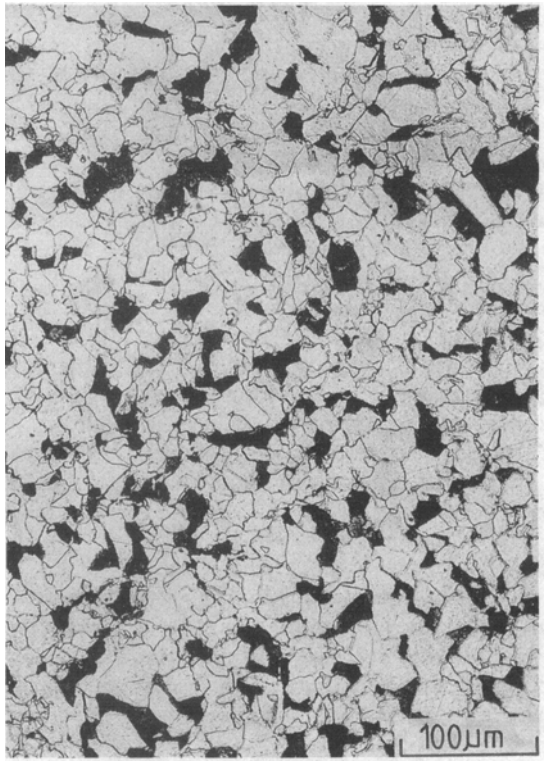

(*c*)

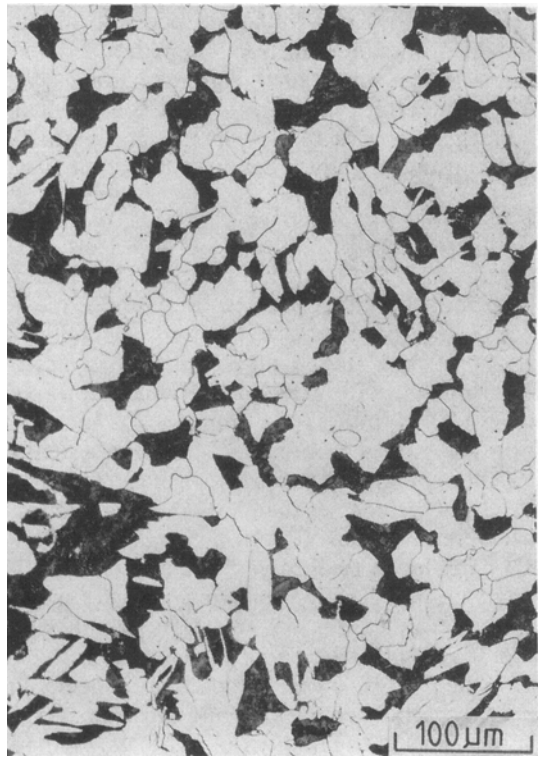

(*d*)

Fig. 2—Light micrographs of steels 2 through 5 cooled at 12 °C/min showing clear polygonal structure: (*a*) steel 2, (*b*) steel 3, (*c*) steel 4, and (*d*) steel 5.

B. *Continuous-Cooling Data*

The extent and morphology of precipitation depended on both temperature and structure. Therefore, in order to assess these in steels 2 and 5, having a mixed structure of bainite, pearlite, and ferrite along with some Widmanstätten ferrite-pearlite, and steels 3 and 4, having some Widmanstätten ferrite-pearlite along with the polygonal structure at the fast cooling rate of 120 °C/min, controlled continuous-cooling dilatometry was carried out on each of the steels at this cooling rate. The transformation start and finish temperatures of steels 2 through 5 at 120 °C/min are presented in Table III. Because the steels cooled at 36 °C/min, 12 °C/min, and 3.6 °C/min produced only polygonal ferrite-pearlite structures, the transformation temperatures were obviously higher and, therefore, controlled cooling dilatometry was not carried out at these slow cooling rates to determine the transformation temperature.

C. *Transmission Electron Microscopy*

Extraction replicas and thin foils were examined to study precipitate morphology and general structural features. Electron diffraction and dark-field microscopy were used to identify the precipitating phases. As the precipitates were often extremely small and the high resolution required to observe them was difficult to obtain in thin foils, due to enhanced spherical and chromatic aberration, extraction replicas were found to provide better information on precipitate morphology. Additionally, there was always the problem of small particles of iron oxides forming on low-alloy steel foils, and both the structure of these oxides and their diffraction pattern confused interpretation when small alloy carbide particles were present.[10,15] Therefore, the thin foils were used mainly to study the general structural features, and extraction replicas were used to study precipitate morphology.

1. *Carbon extraction replica*

Electron micrographs of replicas from the steels cooled at 120 °C/min and 12 °C/min are presented in Figures 3 and 4. They indicate the differences in particle size and distribution. The particle size and the number of precipitates/unit area (mm^2) measured in the electron micrographs obtained from replicas of steels 2 through 5 cooled at 120 °C/min, 36 °C/min, 12 °C/min, and 3.6 °C/min are plotted in Figures 5 and 6 as functions of cooling rate. Figures 5 and 6 show that VC precipitates in steel 2 were coarser than V(C, N) precipitates in steel 3 and were finer than V(C, N) precipitates in steel 4, while AlN particles in steel 5 were the coarsest of all at the cooling rate of 120 °C/min. However, the number of particles/unit area (mm^2) in steel 3 was higher than that in steel 4 and virtually identical with that in steel 2, while that in steel 5 was the lowest of all. As the cooling rate decreased, particle coarsening and growth occurred, causing a reduction in the number of particles/unit area.

Very fine precipitates were found in steels 2 through 4, while steel 5 showed much larger particles. Dark field and high magnification were used to reveal the finest particles in steels 2 through 4. Figure 7 shows the dark-field and high-magnification photographs of the finest particles in steel 2 at 36 °C/min.

Figures 3 and 7 also show that steels 2 and 3 produced some degree of clustering of very fine particles at the fast cooling rates. Both general and interphase precipitation were found in steels 2 and 3 at slow cooling rates, while steel 4 produced some interphase precipitation at all cooling rates. The interphase precipitation in steels 2 and 3 was found less frequently than in steel 4.

The slowly cooled structures were often more heterogeneous than those cooled at 120 °C/min. Inhomogeneity in precipitate morphology was observed in steel 3 at 12 °C/min where the precipitated particles ranged from very fine general precipitate (Figure 4(b)) to large needles of vanadium carbonitride (Figure 8). The heterogeneity in precipitate morphology was also observed in steel 2 at 36 °C/min where some of the precipitates were very fine and some were fairly large. Inhomogeneity was also noticeable in steel 2 at the slowest cooling rate of 3.6 °C/min, where particles ranged from large interphase particles to fine general matrix precipitates. The heterogeneity was particularly pronounced in steel 5 at slow cooling rates, where the AlN particles exhibited very great variations in size and shape (Figure 9).

The precipitates in steel 4 were found to be more uniformly distributed than those in steels 2 and 3 at all cooling rates. Grain boundary precipitates and denuded zones were also observed occasionally in steels 2 through 4, whereas steel 5 did not show denuded zones.

2. *Thin foils*

The microstructural features observed in the thin foils of all the steels are described below.

a. *Microstructure*

Except for steels 2 and 5 cooled at the fastest rate (120 °C/min), the observed microstructures were all essentially mixtures of polygonal ferrite and expected amount of pearlite. Steel 2 showed some acicular ferrite (Figure 10(a)) and a little upper bainite (Figure 10(b)) at the cooling rate of 120 °C/min in addition to the polygonal ferrite-pearlite structure. The bainite content of steel 5 (Figure 10(c)) was found to be relatively high. An unexpected and rare structural feature, twinned martensite, was found in steel 3 at the cooling rate of 120 °C/min (Figure 11(a)). A very small amount of bainite was observed at the slower cooling rates (Figure 11(c)). Another interesting observation was that a very little Widmanstätten ferrite, which is usually formed in coarse-grained material, was also found in this fine-grained steel 3 at the cooling rate of 36 °C/min (Figure 11(b)).

b. *Dislocation density*

A fairly high dislocation density was observed in all the steels at all cooling rates. The dislocation density was found to decrease as the cooling rate decreased. Although steel 3 produced a polygonal ferrite-pearlite structure at all cooling rates, it gave the highest dislocation density of all the steels and also showed an extensive dislocation network. The dislocation density in steel 4 was found to be much lower than in steels 2 and 3, while steel 2 showed a lower dislocation density than steel 3. Figure 12 shows the variation of dislocation density in these three steels. A relatively low dislocation density was observed in steel 5.

c. *Precipitation*

General precipitation was observed at all cooling rates in steels 2 and 3. The precipitates at the fastest cooling rate were found to be very fine in steel 3. Interphase precipitation was also observed frequently at the slowest cooling rate of 3.6 °C/min and less frequently at the cooling rate of 12 °C/min in steel 2 in addition to general precipitation. Figure 13 represents the thin foil micrographs of steel 2, showing general and interphase precipitation at the slow cooling rates.

An important observation is that both general and interphase precipitation were present in the same area in steel 3 at the cooling rates of 36 °C/min and 12 °C/min (Figure 14). The extent of general precipitation was much more than that of interphase precipitation. Precipitation on dislocations and precipitate-dislocation interactions were frequently and extensively found at all the cooling rates (Figure 14), except at the slowest cooling rate of 3.6 °C/min where these features were found less frequently and less extensively.

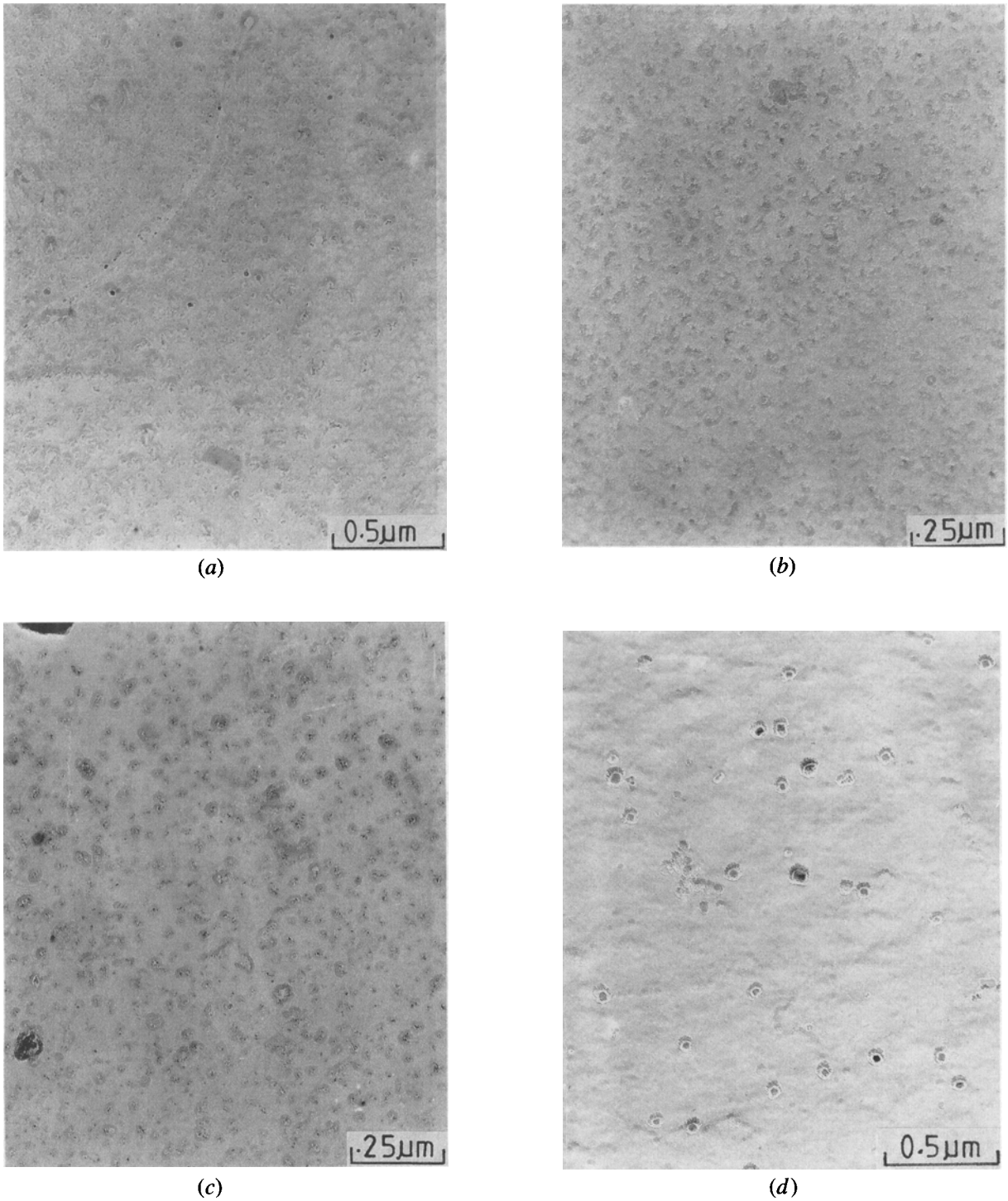

Fig. 3—Carbon extraction replica electron micrographs showing the size and distribution of precipitates of steels 2 through 5 cooled at 120 °C/min: (*a*) steel 2, (*b*) steel 3, (*c*) steel 4, and (*d*) steel 5.

Microscopic study revealed that the size of the precipitates varied from region to region in the same specimen, *i.e.*, some areas had very fine precipitates while other areas had bigger precipitates. The presence of variable particle sizes was thought to be due to the segregation of elements, such as carbon, manganese, and vanadium.

A needlelike morphology of V(C, N) precipitates was occasionally found in steels 3 and 4 at the 12 °C/min cooling rate, as observed with the extraction replicas. Figure 15 illustrates this type of morphology of V(C, N) in steel 3.

Steel 4 contained both general and interphase precipitation at all cooling rates. Figure 16 shows interphase precipitation at the cooling rates of 120 °C/min and 12 °C/min in steel 4. Although general precipitation was found

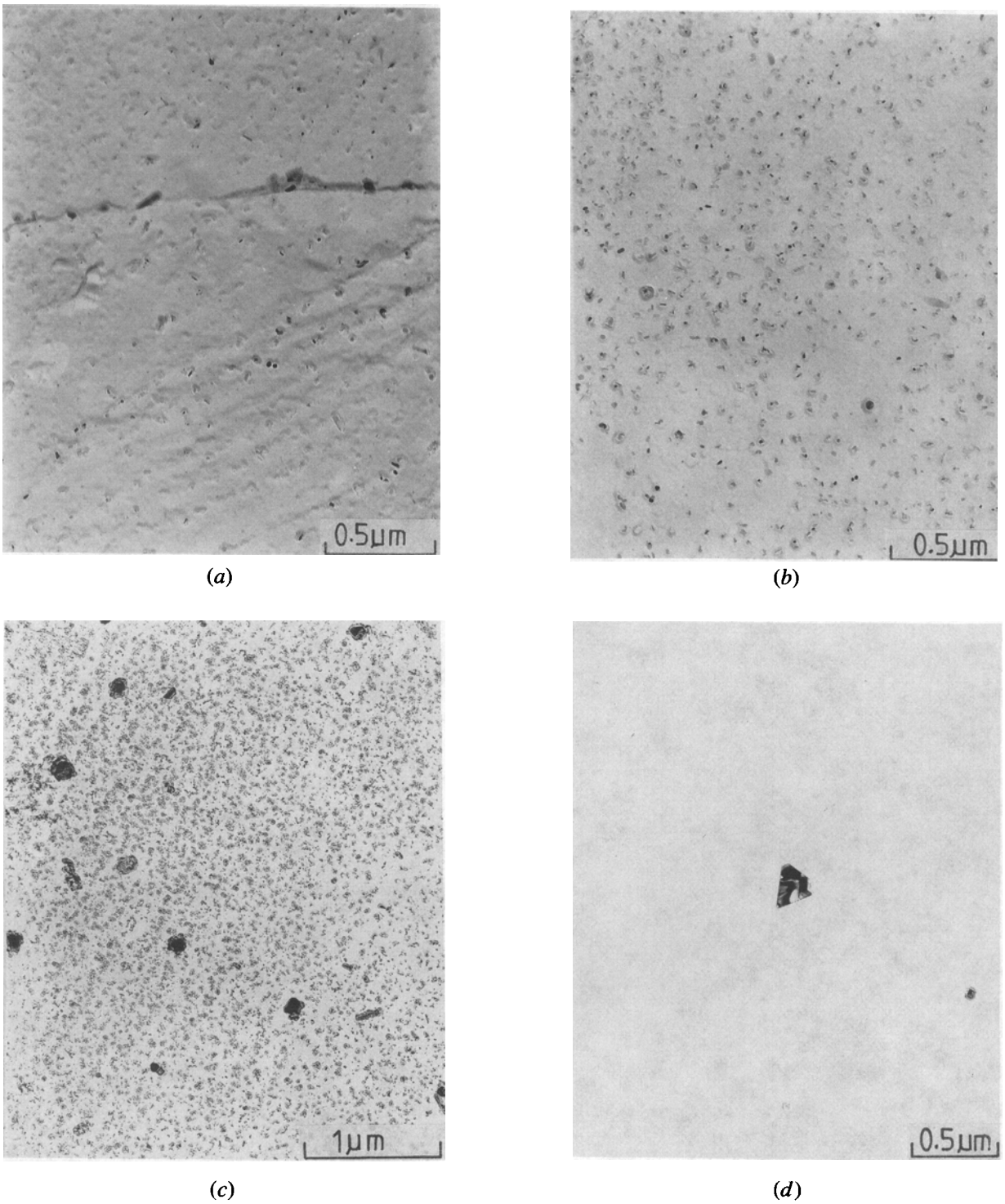

(*a*) (*b*) (*c*) (*d*)

Fig. 4—Carbon extraction replica electron micrographs showing the size and distribution of precipitates of steels 2 through 5 cooled at 12 °C/min: (*a*) steel 2, (*b*) steel 3, (*c*) steel 4, and (*d*) steel 5.

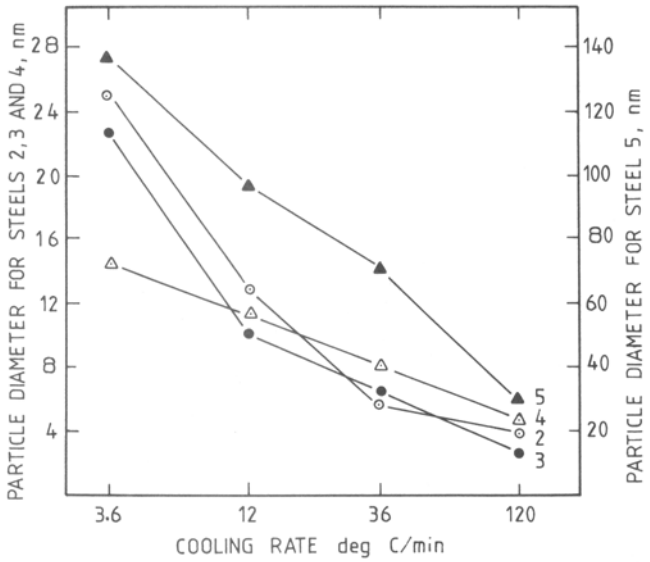

Fig. 5—The variation with cooling rate of the average diameter of the particles of steels 2 through 5.

over large areas, compared to that of interphase precipitation, interphase precipitation was frequently observed in this material. Several dislocations were in contrast (Figure 16), but there was no evidence of long dislocation trails which Suzuki and Tanino[16] claimed to be nucleating sites for V(C, N) interphase precipitation.

The morphology of the lined-up particles observed in the thin foils was similar to that in extraction replicas in steel 4. Typical thin foil micrographs (Figure 17) show that two groups of parallel rows intersect each other.

The size of the particles became coarser as the cooling rate decreased (Figure 5); also, the spacing between the

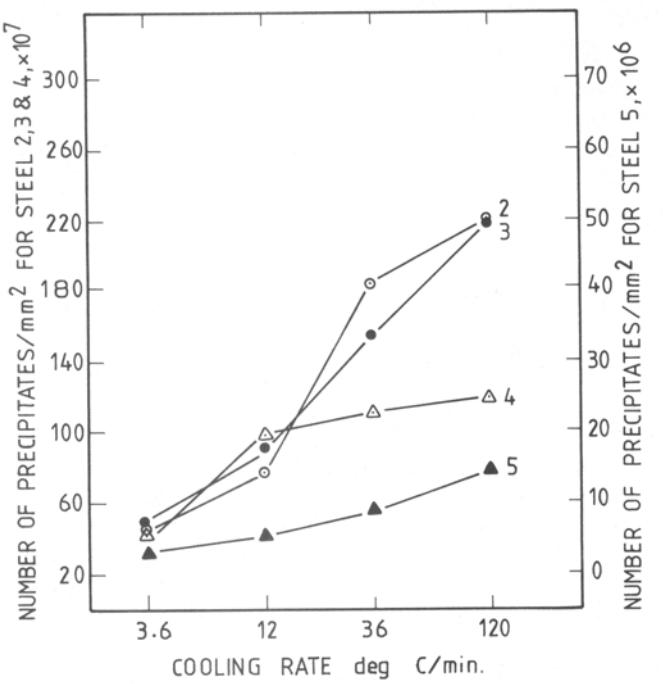

Fig. 6—The variation with cooling rate of the number of precipitates/unit area (mm^2) of steels 2 through 5.

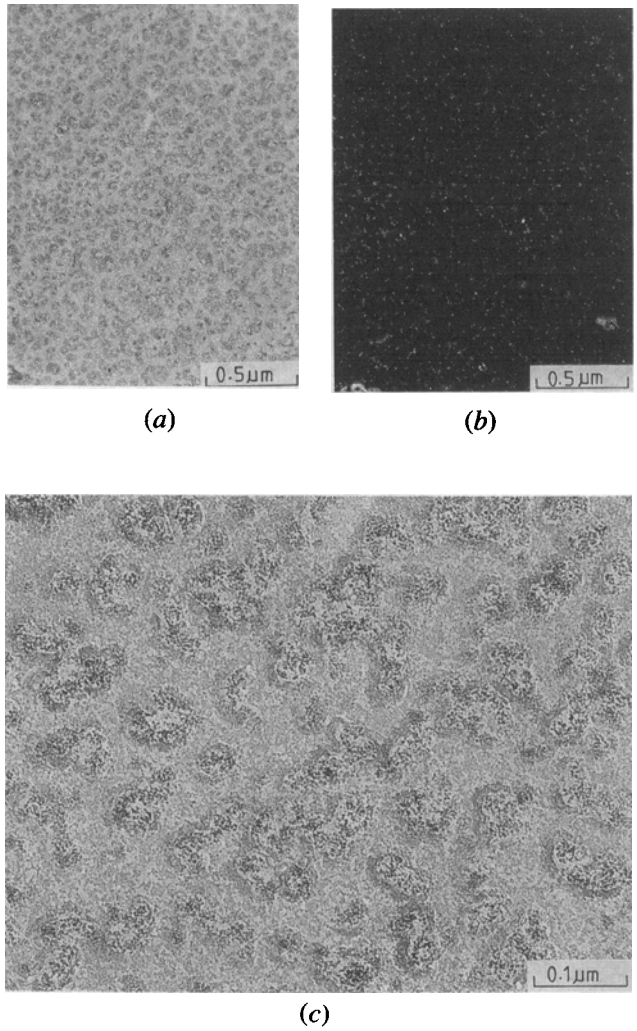

Fig. 7—Typical carbon extraction replica electron micrographs showing the fine vanadium carbide precipitates in steel 2 cooled at 36 °C/min: (*a*) bright field, (*b*) dark field of the same as (a) (using a V(C, N) reflection), and (*c*) bright-field high-magnification micrograph.

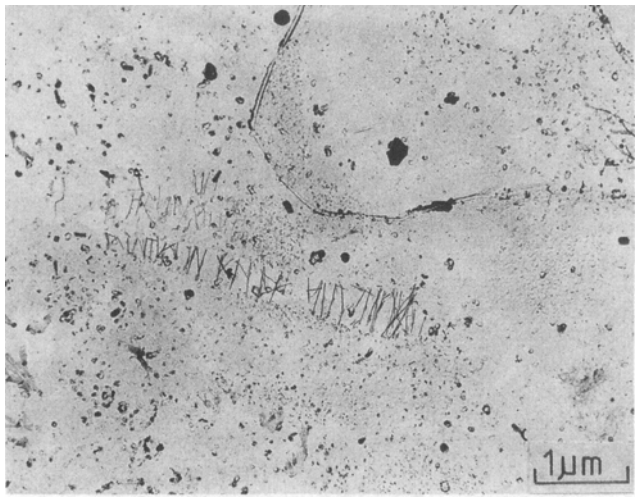

Fig. 8—Carbon extraction replica electron micrograph of steel 3 cooled at 12 °C/min showing the large needle of vanadium carbonitride particles.

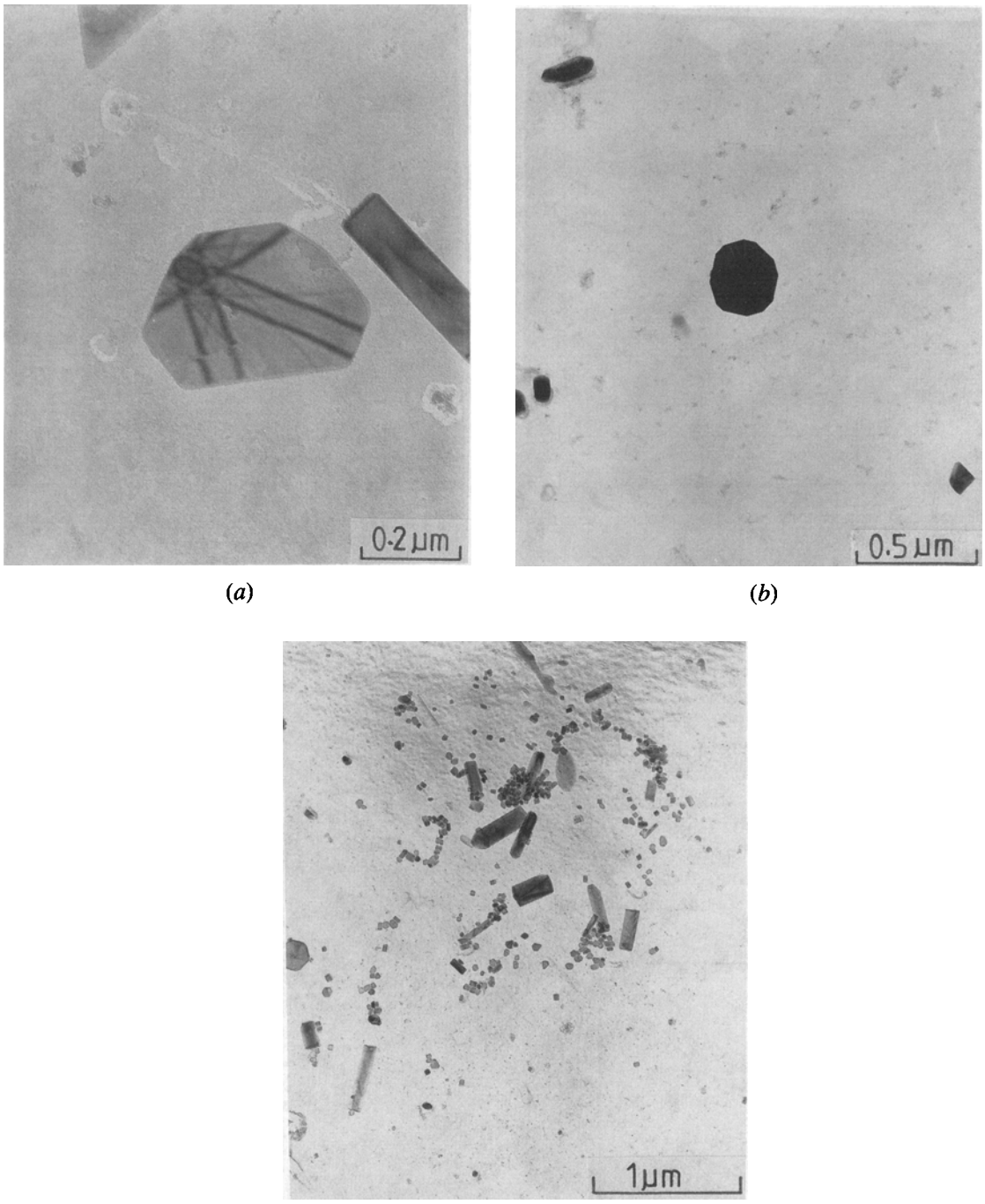

(*a*) (*b*) (*c*)

Fig. 9—(*a*) through (*c*) Carbon extraction replica electron micrographs of steel 5 cooled at 3.6 °C/min showing large rod-type, irregular, and large spherical particles and clusters of relatively smaller particles of AlN.

parallel rows of precipitate increased as the cooling rate decreased.

Another interesting structural feature in steel 4 was the presence of a cluster of AlN particles at the fast cooling rate of 120 °C/min. Figure 18 shows bright-field and dark-field micrographs of the cluster of AlN particles. Moreover, a relatively large number of undissolved, uniformly distributed AlN particles were present in this steel at all cooling rates.

Several morphologies of AlN particles with a great variation in size and shape were also observed in the thin foils of steel 5 at all cooling rates. Grain boundary AlN was also found. No evidence of fine precipitation was found. The thin foil study of this material at the slowest cooling rate of 3.6 °C/min revealed some cluster of AlN particles.

d. *Grain boundary cementite*

Many elongated but thick grain boundary films of cementite were observed in steel 2 at the fastest cooling

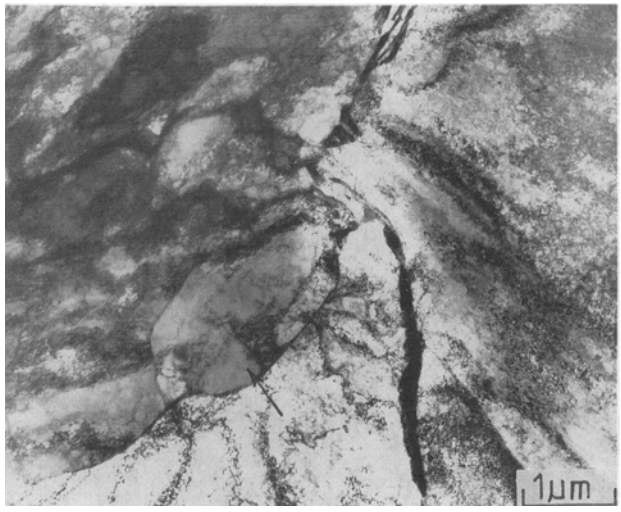

(*a*)

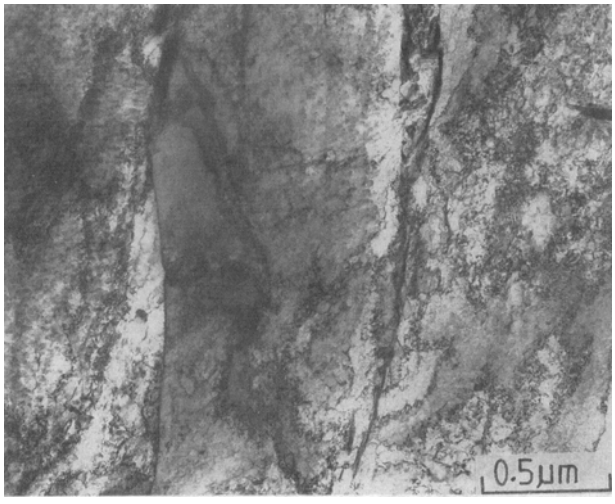

(*b*)

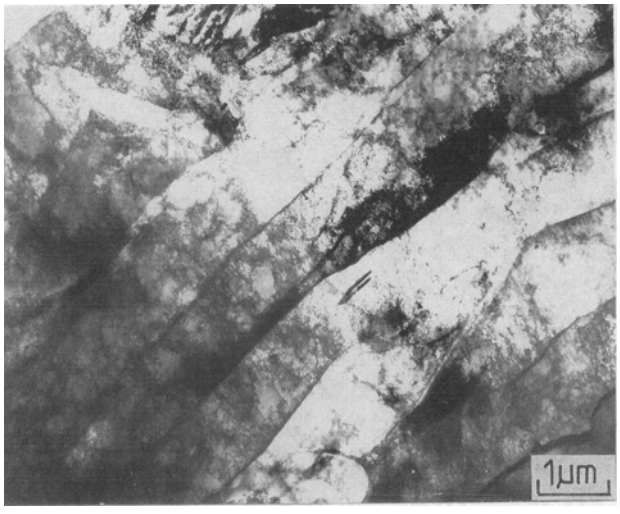

(*c*)

Fig. 10—Typical thin foil electron micrographs showing (*a*) acicular ferrite and (*b*) upper bainite in steel 2 and (*c*) bainitic lath structure in steel 5 cooled at 120 °C/min.

rate of 120 °C/min and in steel 5 at the slowest cooling rate of 3.6 °C/min. A few grain boundary carbides were also observed in steel 5 at 12 °C/min. Steel 3 also produced grain boundary carbides but they were very few in number.

D. *Identification of Precipitates by Electron Diffraction*

Carbon extraction replicas and thin foils of steels 2 through 4 were examined, and ring patterns from the fine precipitates and selected area diffraction patterns of the bigger precipitate phases were recorded. It has already been pointed out that there is always the problem of small particles of iron oxides forming on low-alloy steel foils, and both the structure of the oxide and its diffraction pattern confuse interpretation when small alloy carbide particles are present.[10,15] Carbon extraction replicas, therefore, were used to identify the precipitate particles. The details of the selected area diffraction patterns are presented in Figures 19 and 20. The selected area diffraction patterns of the phases were solved with the aid of computer programs.

Because the lattice parameter of VC varies from 0.4136 to 0.4183 nm and that of VN varies from 0.4097 to 0.4169 nm,[17] it is not possible to differentiate between VC, VN, and V(C, N). The designation V(C, N), therefore, was used above, but it was fairly certain that the second phase in steel 2 was VC and steels 3 and 4 contained V(C, N) as precipitating particles.

Figure 19 shows the $[1\bar{2}1]$, $[0\bar{1}0]$, and $[1\bar{1}0]$ zones of V(C, N). These had a face-centered cubic structure with a lattice parameter of $a_0 \sim 0.416$ nm.

Figure 20 gives the [00.1] and $[\bar{1}1.0]$ zones of AlN; the [00.1] pattern was found frequently in steel 5. This phase was close-packed hexagonal with $a_0 \sim 0.311$ nm and $c_0 \sim 0.499$ nm.

IV. DISCUSSION

Light and electron microscopy confirmed that steels 2 and 5 produced mixed structures of bainite, pearlite, and ferrite at the fastest cooling rate of 120 °C/min, although the volume fraction of bainite in steel 2 was small. Steel 2 was basically a carbon-vanadium steel. The vanadium combined with carbon forming VC and thus reducing the carbon content in solution in the austenite. Because of this lower austenite carbon content, only a little bainite was formed along with ferrite and pearlite. Steel 5 was also basically a carbon steel with aluminum and nitrogen added to it. Because aluminum did not combine with carbon, the total carbon content remained in solution in austenite. This, along with manganese and the additional nitrogen, depressed the transformation temperature to a considerable extent (Table III). As a result, a considerable amount of bainite was found along with ferrite-pearlite in this steel at the fastest cooling rate.

Figure 11(a) showed that steel 3 contained some twinned martensite at the fastest cooling rate of 120 °C/min. The formation of twinned martensite was thought to be due to the segregation of carbon and alloying elements. Twinned martensite usually forms in high-carbon steel,

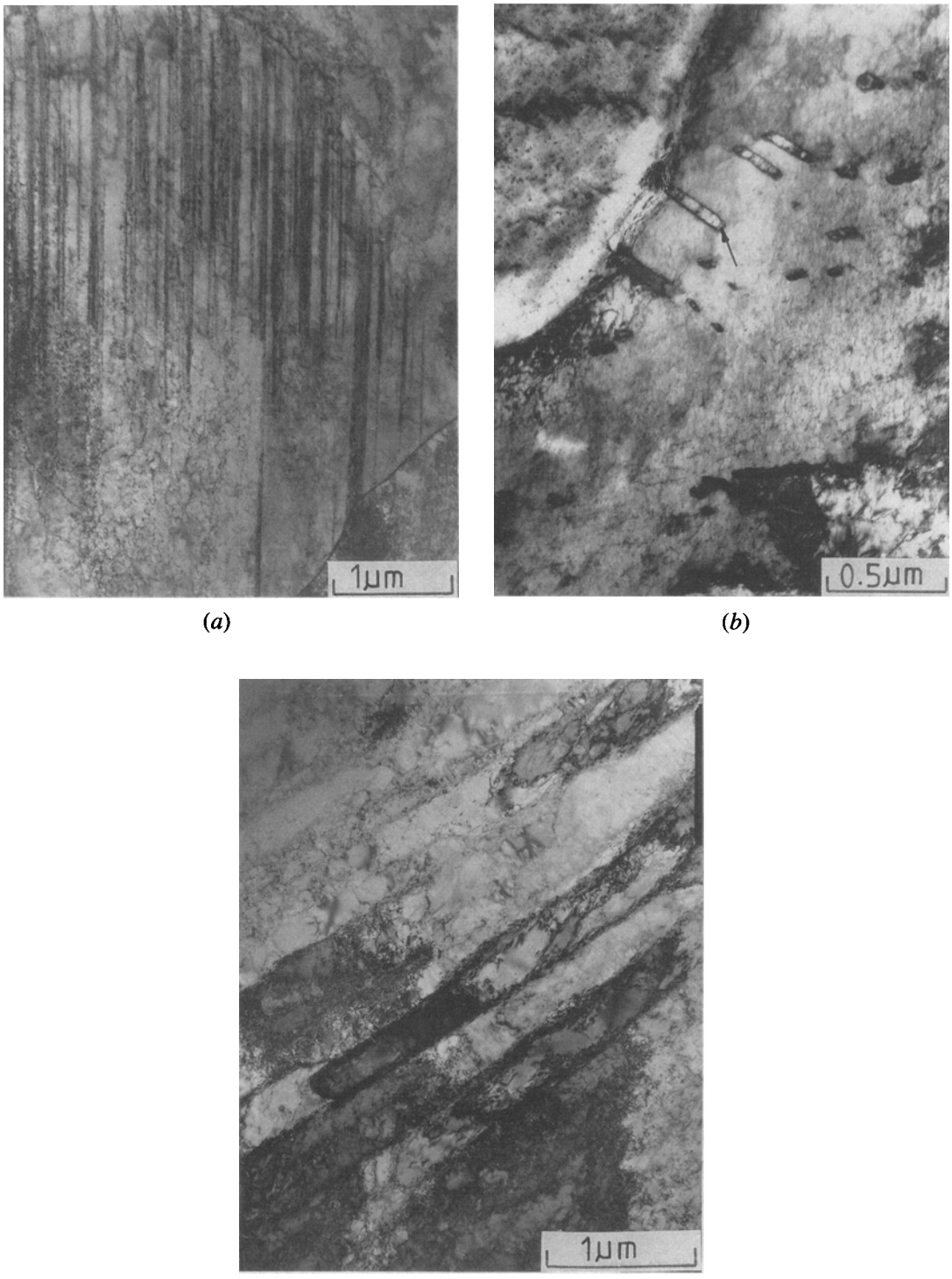

(*a*) (*b*) (*c*)

Fig. 11—Typical thin foil electron micrograph of steel 3 showing (*a*) twin martensite at the cooling rate of 120 °C/min, (*b*) Widmanstätten, *i.e.*, side-plate ferrite at 36 °C/min, and (*c*) lath-type structure (bainite) at 3.6 °C/min.

while lath martensite forms in low-carbon steel. During the $\gamma \rightarrow \alpha$ transformation, concentration of carbon in γ increases gradually and, ultimately, the region of γ which transforms last is richer in carbon and, hence, can transform to twinned martensite if the temperature is low enough and the cooling rate is fast enough.

The reason for the presence of side-plate ferrite in the fine-grained steel 3 (Figure 11(b)) is not clear, as this morphology is usually observed only when ferrite is formed from coarse-grained austenite. The presence of a small amount of bainite in this steel at slower cooling rates (Figure 11(c)) was again thought to be due to the segregation of elements, such as carbon, manganese, and vanadium. Steels 2, 3, and 5 contained some cementite

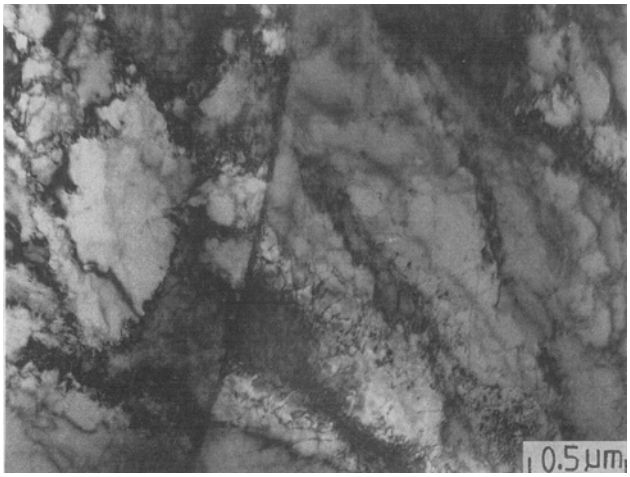

(*a*)

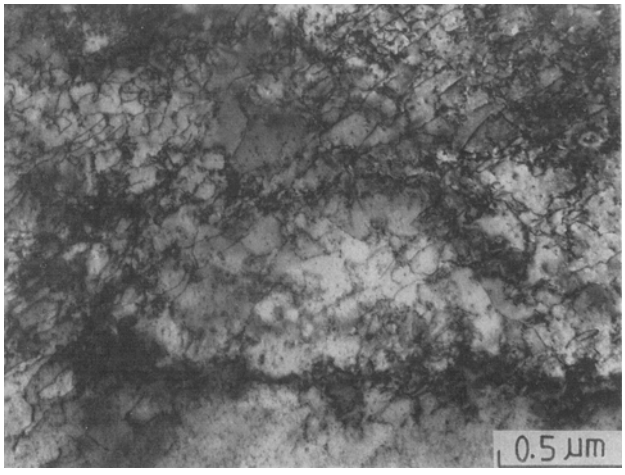

(*b*)

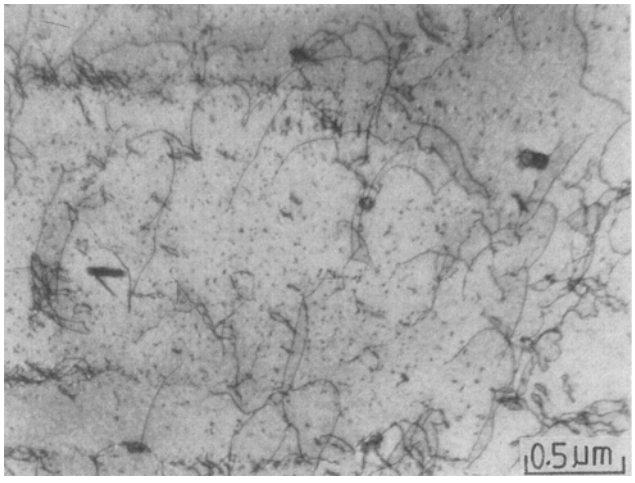

(*c*)

Fig. 12—Typical thin foil electron micrographs of steels 2 through 4 cooled at 120 °C/min showing the variation of dislocation density: (*a*) steel 2, (*b*) steel 3, and (*c*) steel 4.

in the grain boundary. This resulted from the concentration of carbon in the last austenite to transform.

During the $\gamma \rightarrow \alpha$ transformation, dislocations are generated due to transformation stresses. Table III showed that these steels had relatively low transformation temperatures at the highest cooling rate. The dislocations generated at this lower transformation temperature were neither annealed out nor moved to low-energy regions to form a substructure because the temperature was not sufficiently high. Thus, these steels had fairly high dislocation densities. These dislocations act as nucleation sites for the precipitates.[18] The dislocation density of steel 4 with V/N/Al was less than that of steel 3 with V/N (Figure 12) and that of steel 5 with Al/N was also relatively low, indicating clearly that the dislocation density was lower in steels with Al than that in steel without Al.

Because the $\gamma \rightarrow \alpha$ transformation takes place at lower temperatures, for the highest cooling rate, precipitation in the ferrite occurred at lower temperatures and the precipitates had less time to grow. Thus, the precipitates in these steels were much finer than in the lower carbon materials of Niltawach.[10]

A fast cooling rate depresses the transformation temperature and refines the precipitating particles' sizes. Thus, the cooling rate of 120 °C/min was anticipated to give a fine dispersion of small particles and that was, in fact, observed in the experimental work (Figure 5). Figures 5 and 6 and Tables IV and V showed that steel 2 with VC produced a coarser particle size than steel 3 with V(C, N) but a finer particle size than steel 4 with V(C, N) and AlN, while steel 5 with AlN produced the coarsest particle size of all at the cooling rate of 120 °C/min. However, the number of particles/unit area in steel 3 was higher than that in steel 4 and virtually identical with that of steel 2, while that in steel 5 was the lowest of all. The precipitate sizes in steels 2 through 4 were 4.8, 3.5, and 5.6 nm, respectively, indicating that any variation in precipitate size in these steels was not large. However, the precipitate size of steel 5 was 33.4 nm, but it should be noted that this precipitate was an entirely different compound. Vanadium carbide, V_4C_3, precipitates in the temperature range from Ar_3 to about 500 °C.[18] Table III shows the transformation start and finish temperatures of all the steels in the present work for the fastest cooling rate. The transformation start and finish temperatures of steel 2 with VC were 740 °C and 597 °C, respectively, and those of steel 3 with V(C, N) were 716 °C and 572 °C, respectively. Therefore, the precipitates in steel 3 at this cooling rate were expected to be finer than those in steel 2, and this was observed to be the case (Table IV and Figure 5). Steel 4 is basically steel 3 with aluminum added to it. The transformation start and finish temperatures of steel 4 at 120 °C/min were 721 °C and 602 °C, respectively. The transformation finish temperature of this steel was higher than those of steels 2 and 3. The precipitates had more time to grow and, hence, were larger than those in steels 2 and 3 for this cooling rate. Steel 4 also produced a smaller volume fraction of precipitates than steel 3 (Tables IV and V). At the heat-treatment temperature of 1105 °C, the undissolved particles in steel 4 were considered solely as AlN. Because

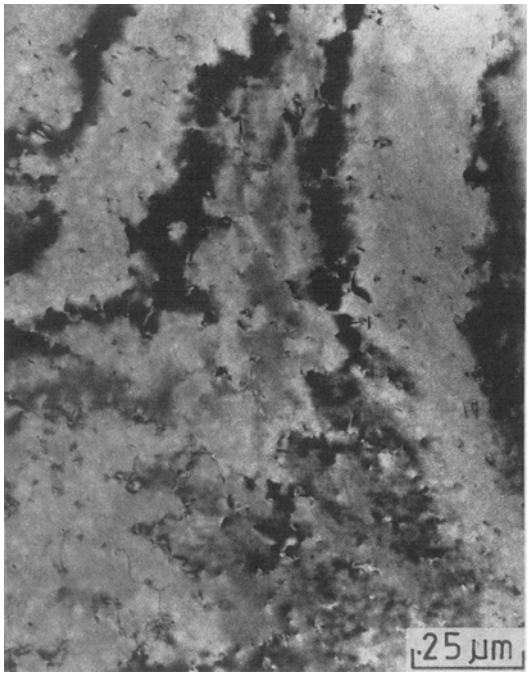

(*a*)

(*b*)

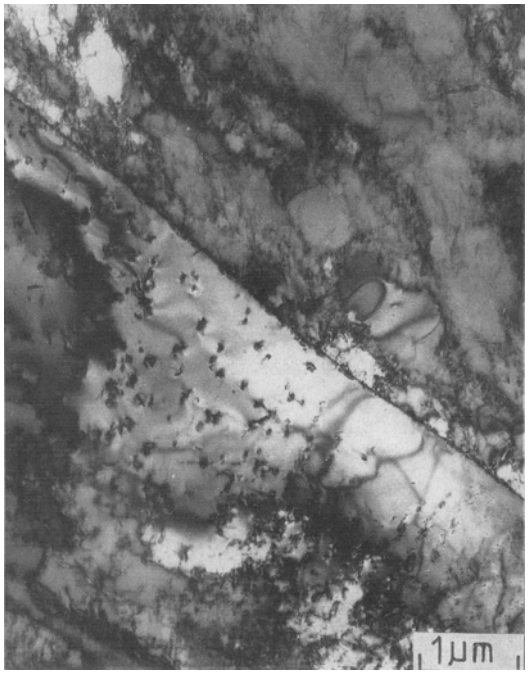

(*c*)

(*d*)

Fig. 13—Typical thin foil electron micrographs of steel 2 showing general and interphase precipitates: (*a*) bright field; cooling rate = 12 °C/min, (*b*) dark field of the same as (a), (*c*) bright field; cooling rate = 3.6 °C/min, and (*d*) bright field showing interphase precipitation; cooling rate = 3.6 °C/min.

of the unfavorable precipitation kinetics of AlN on cooling, the precipitates in steel 4 were assumed to be only V(C, N) and the residual Al was assumed to be in solution. It was thought that in steel 4, the soluble Al affected the kinetics of precipitation of V(C, N), *i.e.*, slowed it down to a sufficient extent to reduce the volume fraction.

As the cooling rate decreased to 36 °C/min, particle coarsening and growth occurred, causing a reduction in the number of particles/unit area (Figures 5 and 6 and Tables IV and V). The extent of particle coarsening will depend on the type and size distribution of the precipitates. Figure 5 indicated that the VC in steel 2 and the V(C, N) in steels 3 and 4 coarsened at a similar rate, indicating that the compositions of the precipitates in these

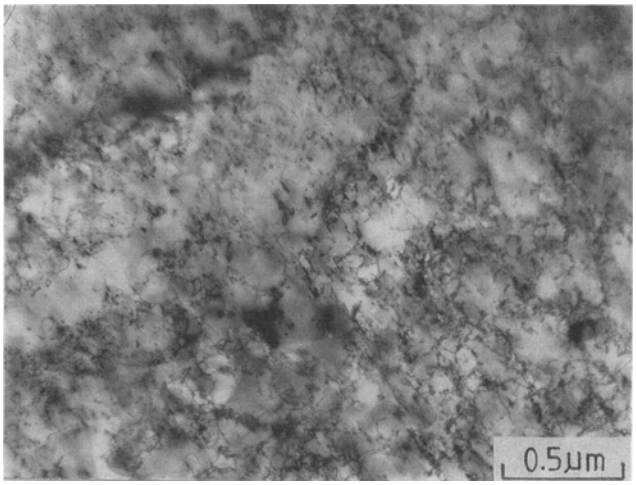

Fig. 14—Typical thin foil electron micrograph of steel 3 cooled at 36 °C/min showing both general and interphase precipitation in one area, precipitation on dislocation, and precipitation-dislocation interaction.

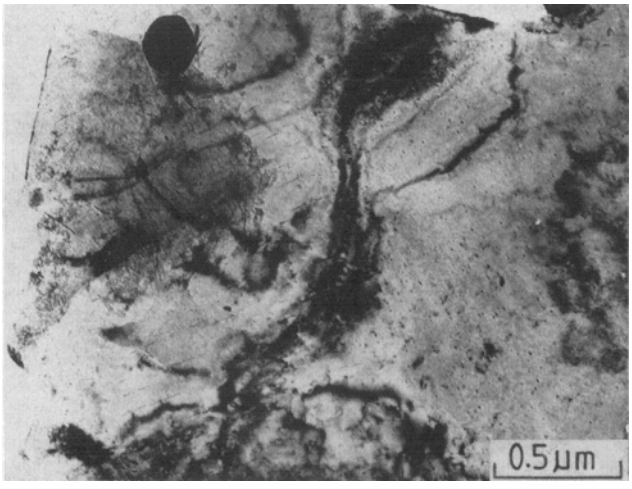

(*a*)

(*b*)

Fig. 15—Bright- and dark-field thin foil electron micrographs of steel 3 cooled at 12 °C/min showing needle-shaped morphology of V(C, N) particles: (*a*) bright field and (*b*) dark field.

(*a*)

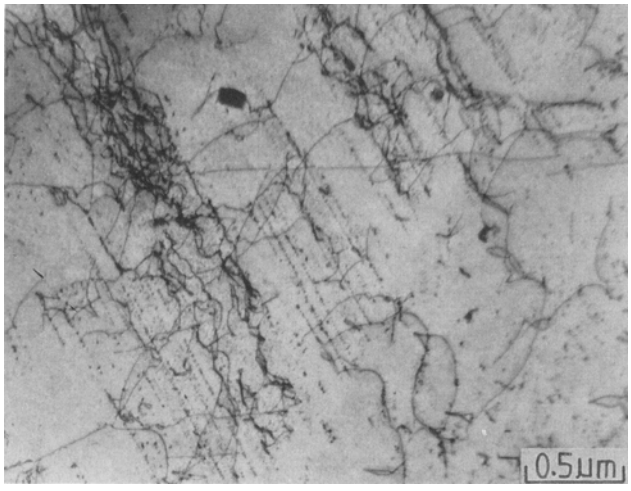

(*b*)

Fig. 16—Typical thin foil electron micrographs showing interphase precipitates at the cooling rate of (*a*) 120 °C/min and (*b*) 12 °C/min in steel 4.

steels were nearly the same. The average precipitate size and the number of precipitates/mm^2 in steel 2 were 6.3 nm and 189 × 10^7, respectively, and those of steel 3 were 7.0 nm and 159 × 10^7, respectively, when cooled at 36 °C/min. From the information about precipitate size and number of precipitates/mm^2, it is evident that these two steels produced similar volume fractions of precipitates. The average precipitate size and number of precipitates/mm^2 for steel 4 were 8.8 nm and 115 × 10^7, respectively, indicating that the volume fraction of the precipitate in this steel was somewhat lower than those of steel 2 or 3.

From Figures 5 and 6, it is evident that particle coarsening and growth occurred with a corresponding decrease in the number of precipitates/mm^2 for all these steels at the cooling rate of 12 °C/min. It is apparent from Figure 5 that the average particle sizes for steels 2 and 3 increased at approximately the same rate with respect to the cooling rate but that this rate was less for steel 4. This again suggests that the compositions of the

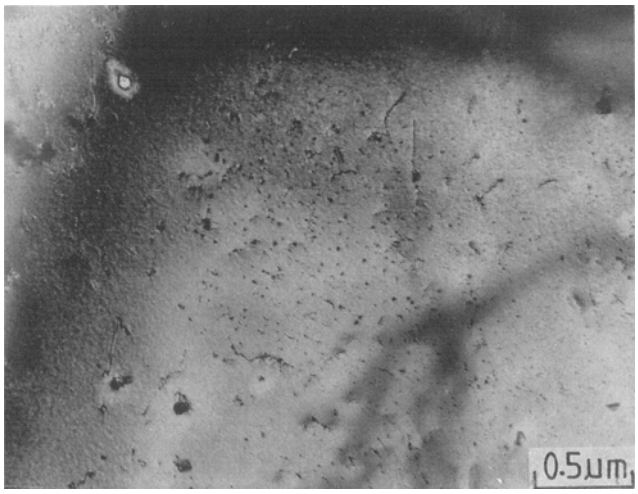

(*a*)

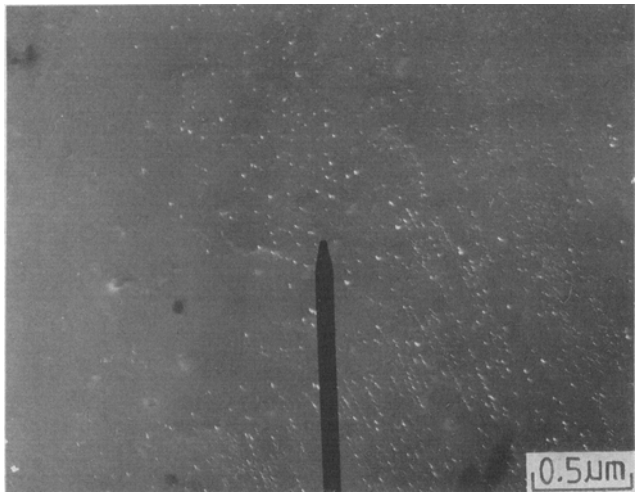

(*b*)

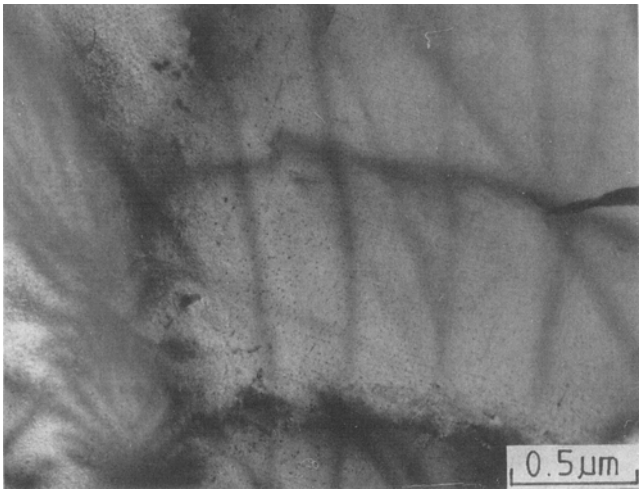

(*c*)

Fig. 17—Typical thin foil electron micrographs of steel 4 showing two groups of parallel rows (lined-up V(C, N) particles) intersecting each other: (*a*) bright field; cooling rate = 12 °C/min, (*b*) dark field of the same as (a), and (*c*) bright field; cooling rate = 120 °C/min.

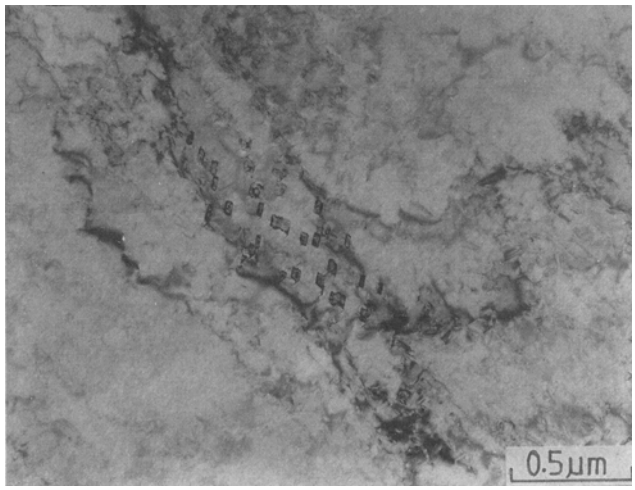

(*a*)

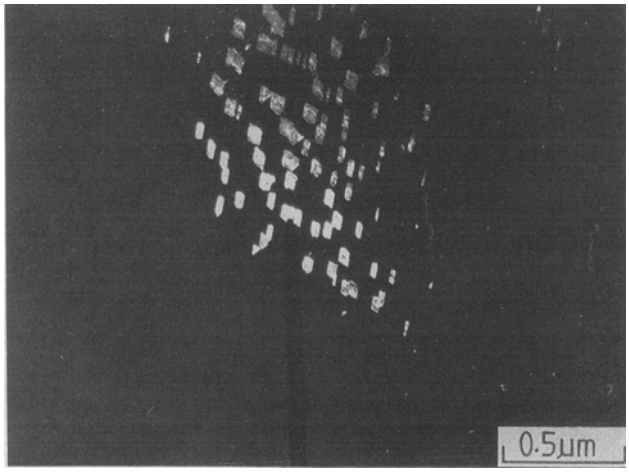

(*b*)

Fig. 18—Typical thin foil electron micrographs of steel 4 cooled at 120 °C/min showing clusters of AlN particles: (*a*) bright field and (*b*) dark field.

precipitates in steels 2 and 3 were similar but different from those in steel 4. Nitrogen analysis confirmed that V(C, N) precipitates formed in steel 4 were higher in nitrogen than those formed in steel 3. The high-nitrogen V(C, N) precipitates were present in a finer dispersion.

At the slowest cooling rate of 3.6 °C/min, it was found that VC in steel 2 and V(C, N) in steel 3 coarsened and grew rapidly but at the same rate, while V(C, N) in steel 4 coarsened much less rapidly. This was thought to be the effect of Al, *i.e.*, Al altered the precipitation kinetics.

Clusters of very fine particles of VC or V(C, N) were present in steels 2 and 3 at the fast cooling rates (Figures 3 and 7). This might be a result of segregation of both vanadium and the interstitial elements which would lead to locally lower transformation temperatures and higher supersaturations.

It was mentioned earlier that severe heterogeneity in the precipitate structures of all steels was found at the slow cooling rates. This was due to the segregation of

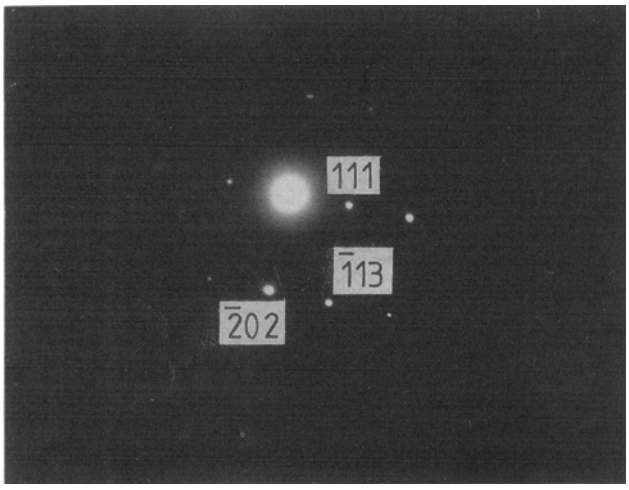

(*a*)

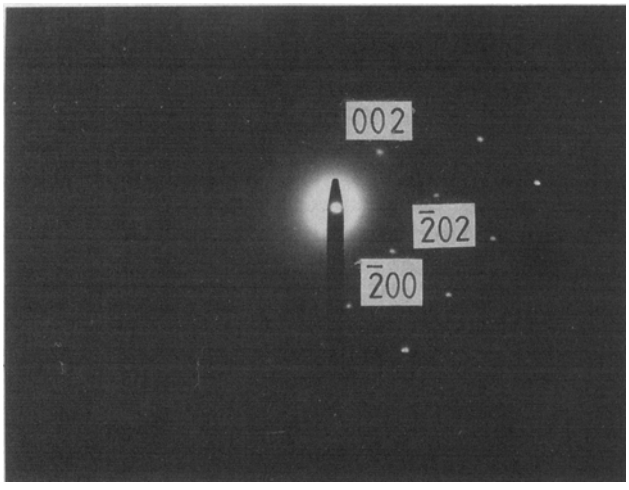

(*b*)

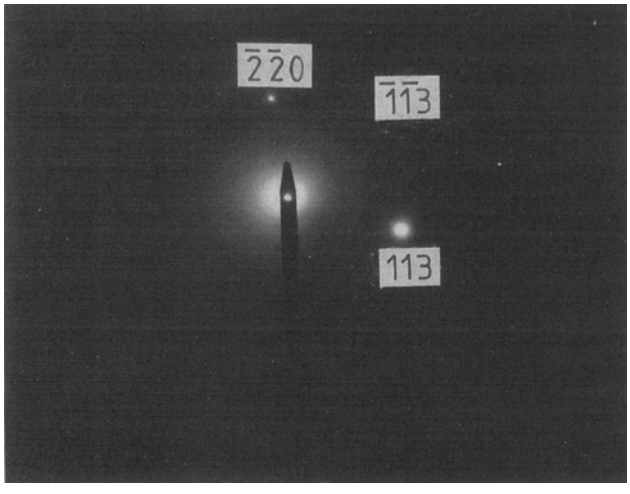

(*c*)

Fig. 19—Diffraction patterns of V(C, N) precipitates. The zone axes are (*a*) [$1\bar{2}1$], (*b*) [$0\bar{1}0$], and (*c*) [$1\bar{1}0$].

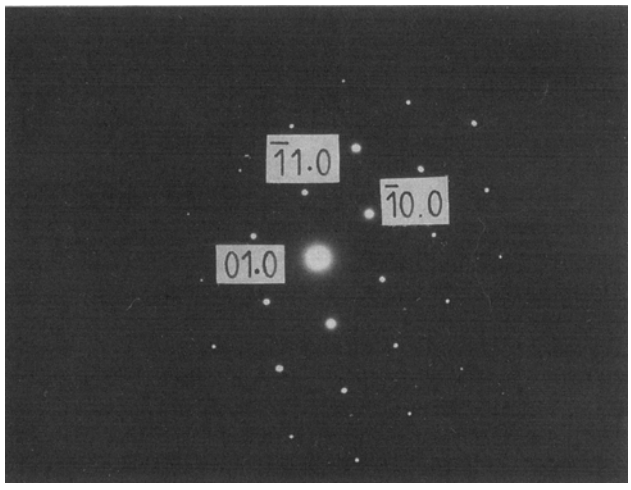

(*a*)

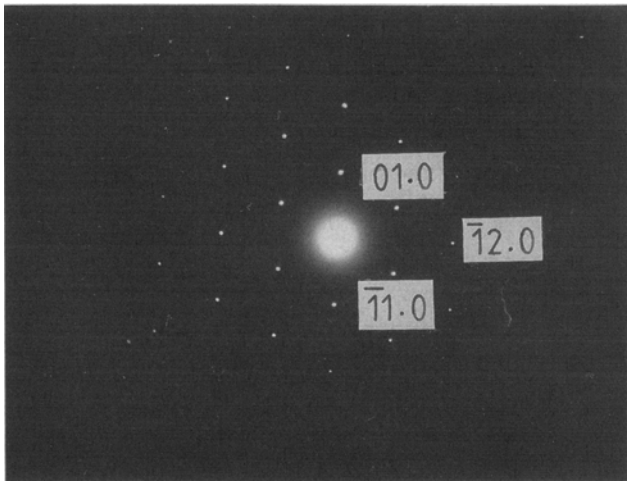

(*b*)

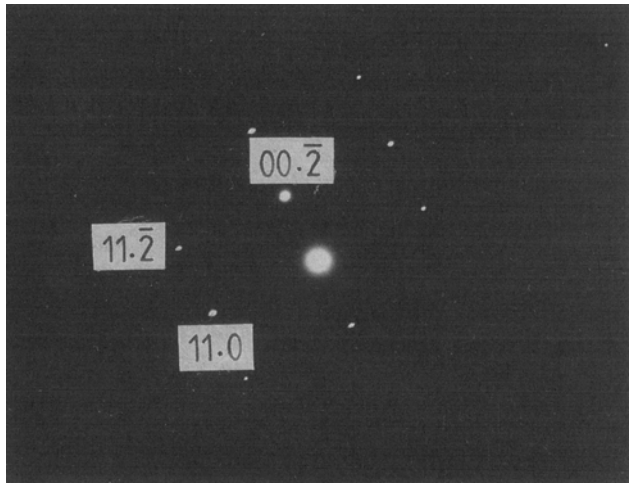

(*c*)

Fig. 20—Diffraction patterns of AlN particles. The zone axes are (*a*) [00.1], (*b*) [00.1], and (*c*) [$\bar{1}$1.0].

Table IV. Average Diameter of the Precipitate Particles of the Steels (nm)

Steel Number	Average Diameter at Four Cooling Rates (°C/min)				Nature of Precipitates
	120	36	12	3.6	
2	4.8	6.3	13.4	25.5	VC
3	3.5	7.0	10.6	22.9	V(C, N)
4	5.6	8.8	11.8	14.7	V(C, N) and AlN
5	33.4	74.0	98.8	138.5	AlN

Table V. Number of Precipitates/Unit Area (mm^2) of the Steels

Steel Number	N_A at Four Cooling Rates (°C/min)			
	120	36	12	3.6
2	226×10^7	189×10^7	81×10^7	46×10^7
3	224×10^7	159×10^7	92×10^7	50×10^7
4	127×10^7	115×10^7	120×10^7	44×10^7
5	16×10^6	10×10^6	6×10^6	3.5×10^6
				$12.5 \times 10^{6*}$

*This figure represents the number of precipitates/mm^2 including the clusters of AlN particles observed at the cooling rate of 3.6 °C/min in steel 5.

elements, like carbon, manganese, and vanadium, and the consequent variation in transformation temperatures.[10]

The average particle sizes of steel 5 at the cooling rate of 120 °C/min and 12 °C/min were 33.4 and 98.8 nm, respectively, and the numbers of particles/unit area at 120 °C/min and 12 °C/min were 16×10^6 and 6×10^6, respectively. Particles of this steel coarsened very rapidly as the cooling rate decreased, and the number of particles reduced accordingly. During cooling, aluminum reacted with nitrogen to form AlN, reducing nitrogen in solution. This AlN did not come out as a precipitate because of its unfavorable precipitation kinetics during subsequent cooling, but it was deposited on the preexisting AlN; hence, the growth of AlN particles was aided. However, at the cooling rate of 3.6 °C/min, this steel produced occasional clusters of AlN particles in a few areas (Figure 9). The number of AlN particles/mm^2 at this cooling rate was 3.5×10^6. This figure rose to 12.5×10^6 when clusters of AlN particles were included. It was thought that these clusters were the result of precipitation during cooling.

The presence of clusters of AlN particles in steels 4 (Figure 18) and 5 (Figure 9) was due to segregation of the element aluminum which combined with nitrogen, forming cluster of AlN particles.

Steel 4 is basically steel 3 with aluminum added to it. It was mentioned earlier that interphase precipitation was observed occasionally in steels 2 and 3 at the slower cooling rates. Steel 4 showed frequent and extensive interphase precipitation along with general precipitation at all cooling rates, although the extent of general precipitation was much greater than that of interphase precipitation, indicating that the presence of aluminum in steel 4 enhanced the formation of interphase precipitates.

The presence of both general and interphase precipitation in the same areas of steel 3 (Figure 14) implied that during the formation of interphase precipitates at the advancing $\gamma \rightarrow \alpha$ boundary, the supersaturation was not wholly relieved.

Bright-field and dark-field thin foil micrographs of steel 4, as shown in Figure 17, showed that two groups of parallel lined-up V(C, N) particles intersected with each other. The boundary between growing ferrite and austenite was made of two portions of the boundary which were aligned at an obtuse angle. As these two segments of the boundary advanced, each left layers of interphase precipitates parallel to itself.

The size of the precipitate particles became coarser as the cooling rate was decreased (Table IV and Figure 5). Also, it is evident from Table VI that the spacing between the parallel rows of interphase precipitates increased as the cooling rate decreased, which is in agreement with the results of Gray and Yeo.[19] The row precipitates (Figures 16 and 17) occurred in ferrite in very thin sheets of particles. The particles within the sheets were randomly arranged. Initially, the particles were considered to be nucleated on dislocations resulting from the volume changes due to the austenite transformation to ferrite.[20,21] It is now firmly established that the nucleation of particles is associated with the austenite/ferrite interface itself, and formation is now described as interphase precipitation.[4–7,19,22] They have suggested that the particles nucleate at the γ/α interface due to the lower solubility of vanadium carbide or carbonitride in ferrite than in austenite. The exact site of nucleation is still open to question. It is difficult to understand how coherent vanadium carbide precipitates can retain coherency when

Table VI. Average Spacing between the Parallel Rows of Interphase Precipitates in Steel 4

Cooling Rate (°C/min)	Average Spacing between Rows of Particles (nm)
120	19.5
36	24.0
12	41.5
3.6	47.5

nucleated heterogeneously on a moving interface.[23,24] However, as vanadium carbide or carbonitride particles have a platelike habit and a unique orientation relationship with ferrite, it is agreed that they nucleate on the ferrite side of the γ/α interface and result in a depletion of the adjacent austenite in carbon.[7] The γ/α interface then moves further into γ, and repeated nucleation of the alloy carbide/carbonitride occurs. In some instances, steps or ledges are seen in the interface, and it has been suggested that interphase precipitation occurs entirely by lateral movement of coherent vertical steps or ledges.[7] However, this mechanism would not appear to satisfy all observations of interfaces in microalloyed steels.[25]

V. CONCLUSIONS

1. In the steels studied, the microstructure was essentially a polygonal ferrite-pearlite structure, except for steel containing vanadium and that containing aluminum and nitrogen cooled at the fastest rate. At this cooling rate, these two steels produced a mixed structure of bainite, pearlite, and ferrite, but the volume fraction of bainite was small. Acicular ferrite, twinned martensite, and Widmanstätten ferrite were also present in some steels at certain cooling rates.
2. The dislocation density was fairly high in all the steels at all cooling rates. The dislocation density decreased as the cooling rate decreased. The dislocation density was lower in the steels containing aluminum than in the steels without aluminum.
3. Because of the low transformation temperatures of the fastest cooling rate, all the steels, except the steel containing only aluminum and nitrogen, produced very fine precipitates.
4. At the fast cooling rates, the segregation of both vanadium and interstitial elements, which produced locally lower transformation temperatures and higher supersaturations, resulted in clusters of fine particles of V(C, N). The heterogeneity was particularly pronounced in the steel containing only aluminum and nitrogen at the slower cooling rates, where the AlN particles showed a wide variation in size and shape. A needlelike morphology of V(C, N) precipitates was occasionally found in the slowly cooled steels containing either vanadium and nitrogen or vanadium, nitrogen, and aluminum.
5. In low-carbon (0.15 pct) structural steels containing vanadium, nitrogen, and aluminum separately or together, the extent of general precipitation was much greater than interphase precipitation, although interphase precipitation was found frequently at the slower cooling rates.
6. The presence of aluminum enhanced the formation of interphase precipitates of V(C, N) at all cooling rates, and the spacing between parallel rows of precipitates increased as the cooling rate decreased.
7. As the supersaturation was not wholly relieved during the formation of interphase precipitates at the advancing boundary, both general and interphase precipitation were present in the same area.
8. The coarsening rate of V(C, N) in the presence of aluminum was considerably lower than that of VC or of V(C, N) in the absence of aluminum.
9. Because of the unfavorable precipitation kinetics, AlN formed during cooling did not nucleate separately but was deposited on the pre-existing AlN particles, thus causing them to be coarsened very rapidly with decreasing cooling rate.

ACKNOWLEDGMENTS

The author is grateful to Mr. J.H. Woodhead, Senior Lecturer, Department of Metallurgy, University of Sheffield, England, for his supervision of this research work. The author wishes to thank Professors G.W. Greenwood and G.J. Davies, Department of Metallurgy, University of Sheffield, for the provision of research facilities. The author expresses his gratefulness to the Association of Commonwealth Universities, London, for the Scholarship and Bangladesh University of Engineering and Technology, Dhaka, for the study leave during the period of this research.

REFERENCES

1. E. Tekin and P.M. Kelly: *Precipitation from Iron-Based Alloys*, AIME Conf. Proc., Gordon and Breach, New York, NY, 1965.
2. E. Tekin and P.M. Kelly: *J. Iron Steel Inst.*, 1965, vol. 203, p. 715.
3. E. Smith: *Acta Metall.*, 1966, vol. 14, p. 583.
4. J.H. Woodhead and D. Webster: *J. Iron Steel Inst.*, 1969, vol. 207, p. 51.
5. A.T. Davenport, F.G. Berry, and R.W.K. Honeycombe: *Met. Sci. J.*, 1968, vol. 2, p. 104.
6. F.G. Berry, A.T. Davenport, and R.W.K. Honeycombe: *Mechanism of Phase Transformations in Crystalline Solid*, Institute of Metals, 1969, Monogr. No. 33, p. 288.
7. A.T. Davenport and R.W.K. Honeycombe: *Proc. R. Soc.*, 1971, vol. A322, p. 191.
8. H.C. Sutton and J.A. Whiteman: *J. Iron Steel Inst.*, 1971, vol. 209, p. 220.
9. M. Tanino, T. Nishida, T. Oaka, and K. Yoshikawa: *Proc. Symp. on Micrometallurgy*, Jamshedpur, India, 1965, p. 77.
10. S. Niltawach: Ph.D. Thesis, University of Sheffield, Sheffield, England, 1977.
11. M.M.A. Bepari: Ph.D. Thesis, University of Sheffield, Sheffield, England, 1981.
12. M.M.A. Bepari: *Metall. Trans. A*, 1989, vol. 20A, pp. 13-16.
13. M.M.A. Bepari: *Mater. Sci. Technol.*, 1989, vol. 5, pp. 13-19.
14. M.M.A. Bepari: *Mater. Sci. Technol.*, 1990, vol. G, pp. 338-48.
15. S.R. Keown and D.J. Dyson: *J. Iron Steel Inst.*, 1966, vol. 204, p. 832.
16. H.G. Suzuki and M. Tanino: *Trans. Iron Steel Inst. Jpn.*, 1972, vol. 12, p. 217.
17. K. Aoki and M. Tanino: *Yawata Technical Report*, 1966, vol. 225, pp. 6550 and 6678.
18. M. Tanino, H.G. Suzuki, and K. Aoki: *Trans. Jpn. Inst. Met.*, 1968, vol. 9, p. 393.
19. J.M. Gray and R.B.G. Yeo: *Trans. ASM*, 1968, vol. 61, p. 255.
20. W.B. Morrison: *J. Iron Steel Inst.*, 1963, vol. 201, p. 317.
21. M. Tanino and K. Aoki: *Trans. Iron Steel Inst. Jpn.*, 1968, vol. 8, p. 337.
22. S. Freeman: *Effect of Second-Phase Particles on the Mechanical Properties of Steel*, The Iron and Steel Institute, London, 1971, pp. 152 and 205.
23. T.N. Baker: *J. Iron Steel Inst.*, 1973, vol. 211, p. 502.
24. T.N. Baker and A.J. Lapointe: *Proc. EMAG 77*, Institute of Physics, London, 1977, p. 195.
25. T.N. Baker: *Sci. Prog., Oxford*, 1978, vol. 65, p. 493.